Title

Nitrogen isotopes reveal high NOx emissions from arid agricultural soils in the Salton Sea Air Basin

Journal

Scientific Reports, 14(1)

ISSN

2045-2322

Authors

Lieb, Heather C

Maldonado, Matthew

Ruiz, Edgar

et al.

Publication Date

2024

DOI

10.1038/s41598-024-78361-y

Peer reviewed

scientific reports

Check for updates

OPEN

Nitrogen isotopes reveal high NO_x emissions from arid agricultural soils in the Salton Sea Air Basin

Heather C. Lieb[1], Matthew Maldonado[2], Edgar Ruiz[2], Christian Torres[2], Luis Olmedo[2], Wendell W. Walters[3] & Ian C. Faloona[1]✉

Air quality management commonly aims to mitigate nitrogen oxide (NO_x) emissions from combustion, reducing ozone (O_3) and particulate matter (PM) pollution. Despite such ongoing efforts, regulations have recently proven ineffective in rural areas like the Salton Sea Air Basin of Southern California, which routinely violates O_3 and PM air quality standards. With over $2 billion in annual agricultural sales and low population density, air quality in the region is likely influenced by the year-round farming activity. We conducted a source apportionment of NO_x (an important precursor to both O_3 and PM) using nitrogen stable isotopes of ambient NO_2, which revealed a significant contribution from soil-emitted NO_x to the regional budget. The soil source strength was estimated based on the mean $\delta^{15}N$-NO_x from each emission category in the California Air Resources Board's NO_x inventory. Our annual average soil emission estimate for the air basin was 11.4 ± 4 tons/d, representing ~ 30% of the extant NO_x inventory, 10× larger than the state's inventory for soil emissions. Unconstrained environmental factors such as nutrient availability, soil moisture, and temperature have a first-order impact on soil NO_x production in this agriculturally intensive region, with fertilization and irrigation practices likely driving most of the emissions variability. Without spatially and temporally accurate data on fertilizer application rates and irrigation schedules, it is difficult to determine the direct impacts that these variations have on our observations. Nevertheless, comparative analysis with previous studies indicates that soil NO_x emissions in the Imperial Valley are likely underrepresented in current inventories, highlighting the need for more detailed and localized observational data to constrain the sizeable and variable emissions from these arid, agricultural soils.

Nitrogen oxides ($NO_x = NO + NO_2$) are a precursor to ozone (O_3) and particulate matter (PM), both of which are federally regulated criteria pollutants known to negatively impact human health and the environment[1]. NO_x is produced through natural, biogenic, and anthropogenic processes, although a critical distinction is necessary. Natural sources of NO_x occur without influence from human activity, such as lightning or weather-induced wildfires. Biogenic NO_x is naturally occurring and is produced by living organisms through microbial nitrification/denitrification cycles in soils. Further, anthropogenic NO_x results from human activities such as fossil fuel combustion in vehicles and power plants. However, these natural processes can be affected by anthropogenic activity, such as biomass burning in agricultural systems, human-ignited wildfires in poorly managed landscapes, and microbial activity in soils of fertilized croplands.

Anthropogenic combustion sources have traditionally been the primary focus of air quality management practices, as they have historically been the dominant source of NO_x emissions, with biogenic processes accounting for ~ 20% of the global NO_x budget, on average[2–8]. These practices have largely reduced precursor emissions, yet several of the United States' worst-air quality districts remain in rural regions[9,10], including the Imperial and Coachella Valleys of Southern California. Together these valleys constitute the Salton Sea Air Basin (SSAB, Fig. 1), which is currently nonattainment for the O_3, $PM_{2.5}$, and PM_{10} National Ambient Air Quality Standards (NAAQS). Interregional transport from larger metropolitan areas is often blamed[11–16], hewing to the traditional paradigm of combustion dominant sources. This issue is a serious matter of environmental injustice because residents of Imperial County are 86% Latino and 21% of residents live below the poverty line[17]. Additional burdens these communities face include high rates of asthma, insufficient housing availability and poor infrastructure, language barriers, and impaired water quality[18,19]. These factors put residents at risk of respiratory damage and diseases like asthma and COVID-19[20]. In fact, Imperial County held both the

[1]Department of Land, Air, and Water Resources/Air Quality Research Center, University of California, Davis, California, USA. [2]Comité Cívico del Valle, Brawley, California, USA. [3]Department of Chemistry and Biochemistry, University of South Carolina, Columbia, South Carolina, USA. ✉email: icfaloona@ucdavis.edu

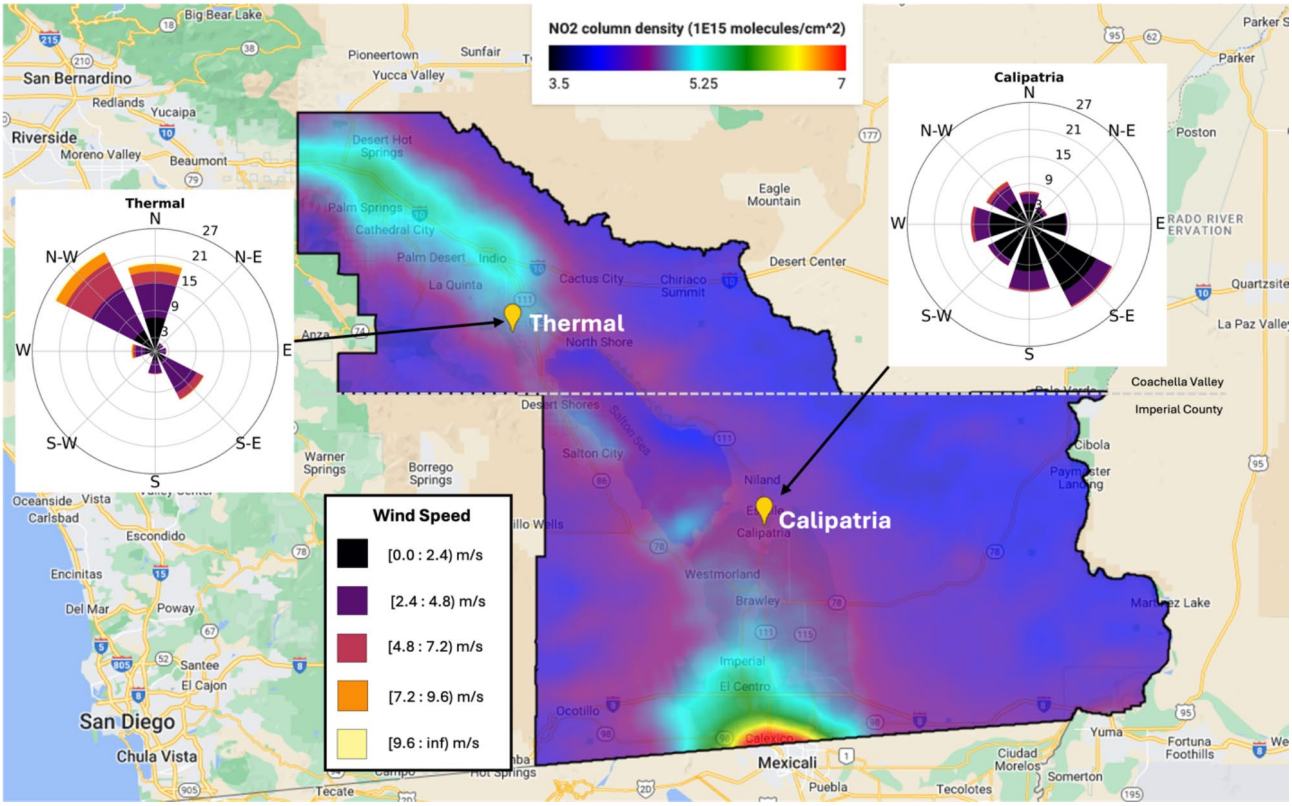

Fig. 1. NO_2 column density was averaged from June 1, 2022, to May 31, 2023, from TROPOMI satellite data for the Salton Sea Air Basin to show the average spatial variation of NO_2. Calipatria (SE) and Thermal (NW), our two sampling sites, are indicated by a yellow marker. Wind roses for Calipatria and Thermal are overlaid on the map and were created using CARB's Meteorological Data Query Tool https://www.arb.ca.gov/aqmis2/metselect.php. The map was created in Google Earth Engine using the Sentinel-5P NRTI NO_2: Near Real-Time Nitrogen Dioxide dataset; the script to access this data was modified but the original script can be found at this link: https://developers.google.com/earth-engine/datasets/catalog/COPERNICUS_S5P_NRTI_L3_NO2.

highest infection and mortality rates per capita in California from COVID-19 throughout the height of the pandemic[21,22]. Members of the rural Eastern Coachella Valley also suffer from similar socioeconomic and environmental injustices[19].

The SSAB is an agriculturally active desert responsible for over $2 billion in annual agricultural sales due to mild temperatures and abundant sunshine in the winter, allowing for year-round production[23]. However, growing crops in sandy soil is challenging and can require anthropogenic land modifications such as carbon-based amendments, heavy application of inorganic fertilizers, and intensive irrigation. This is primarily due to the soil's texture, with larger particle diameters and lower organic carbon composition, resulting in poor retainment of water and nutrients necessary for plant growth[24]. Tillage is often required for agricultural production in sandy soils, which can result in structural damage to the soil, leading to compacted soils that are difficult to cultivate when dry, as well as entrainment of particulate matter[24–26]. Hard-setting soils have high soil strength that is not suitable for root growth or shoot development. Consequently, this requires frequent soil-wetting through irrigation practices, especially in summer months when temperatures regularly exceed 35 °C; these dry, hot conditions and changes in volumetric soil moisture (VSM) may lead to large, transient soil NO_x emissions (Fig. 1 & S1)[10,24,27].

In addition, inorganic fertilizer amendments are not regulated, leading to over-application and nutrient leaching into the surrounding environment, such as the groundwater, local water sources, atmosphere, and soils[24,28]. The objective of this work is to understand the implications of agricultural practices in arid agroecosystems of the SSAB on regional air quality. Observations and modeling studies show a massive expansion of arid lands globally due to climate change, with estimates ranging from 2.5 to 6.5 million km^2 by the end of the century, especially in large croplands in the northern hemisphere[29]. Consequently, agricultural production in arid ecosystems will become more prominent[30], therefore the implications of these practices need to be better understood. Microbes in soils naturally produce nitric oxide (NO), nitrous oxide (N_2O), and nitrous acid (HONO) gases during nitrification and denitrification processes, but their relative amounts are highly uncertain. These processes are dependent on many variables, but most importantly on the availability of reactive nitrogen and molecular oxygen, nitrifying and denitrifying bacteria, soil moisture and pH, and temperature[31–35]. Nitrification is a multi-step microbial process (shown below separated into 2 steps) that converts available ammonia (NH_3) into nitrate (NO_3^-) and involves ammonia-oxidizing and nitrite-oxidizing bacteria[36]. NO

can be a byproduct in Step 1 under high ammonia concentrations or low oxygen conditions. Irrigation and precipitation events temporarily suppress bacterial activity until water is redistributed or evaporated, restoring oxygen and nutrient availability and resulting in NO pulsing events.

$$NH_3 + O_2 \rightarrow NO_2^- + H_2O + H^+ \quad \text{(Step 1)}$$

$$NO_2^- + O_2 \rightarrow NO_3^- \quad \text{(Step 2)}$$

Denitrification (Step 3) is a sequence of biochemical reactions that reduce nitrate to dinitrogen (N_2) and other gaseous products (e.g., HONO, NO, N_2O), typically occurring under anaerobic conditions when bacteria use nitrate as an oxidizing agent in the absence of oxygen[37]. In this process, NO is an intermediate and can be emitted when there is an imbalance in electron donors and acceptors (e.g., not enough organic carbon) or under acidic soil conditions where denitrifying bacterial activity is inhibited. However, in this step N_2O emissions are believed to dominate over NO particularly in wetter soils.

$$NO_3^- \rightarrow NO_2^- \rightarrow NO \rightarrow N_2O \rightarrow N_2 \quad \text{(Step 3)}$$

In agricultural soils the availability of reactive N in the form of NH_4^+ and NO_3-, which fuels these nitrification/denitrification reactions, is directly dependent on N fertilizer inputs, meaning overapplication of N fertilizers results in emissive nitrogen gases. Applying excessive ammonia-based fertilizer with insufficient oxygen availability (e.g., when fields are flooded) can result in NO production from nitrification because nitrite is not able to fully oxidize to nitrate. In addition, soil texture influences the relative proportions of N gases released from nitrification and denitrification; denitrification is favored in clay soils while nitrification is favored in freely draining sandy soils, like the ones in the SSAB[38,39]. Soil NO emissions are observed to increase exponentially with temperature due to enzymatic activity and microbial turnover rates, then plateau between 30 and 40 °C, as long as these other soil components are not limiting factors[34,40,41]. The exact temperature that these emissions plateau is still debated, however, we believe that the plateau point may be higher in hot agroecosystems like the SSAB, where microbes have likely adapted to the extreme heat[42].

Further, high pH soils are generally believed to favor microbial ecosystems that promote nitrification and NO production, while acidic soils produce HONO through chemical equilibrium with nitrite in water[34]. However, Oswald et al. (2013) found comparable quantities of HONO and NO emitted from nonacidic soils, suggesting that HONO may be an unaccounted, yet significant amount of reactive nitrogen released from soil worldwide, particularly dominant in arid and arable environments like the SSAB. This is crucial as the lifetime of HONO with respect to photolysis yielding NO + OH is around 15 min during the daytime, causing soil emissions to rapidly cycle into the photostationary state of O_3-NO-NO_2, becoming an additional source of NO_x to the atmosphere[43].

As NO_x emissions from combustion sources decline under ongoing air quality regulations, it becomes crucial to comprehend the impact of anthropogenically induced biogenic NO_x production, particularly from agricultural soils. The nitrogen stable isotope composition ($\delta^{15}N$) is proposed as a valuable tool for NO_x source apportionment due to differences in mean $\delta^{15}N$-NO_x values between anthropogenic and biogenic emission sources[44–46]. Ambient $\delta^{15}N$-NO_2 is recognized as an effective means of source apportionment, benefiting from well-quantified isotope fractionation factors and offsetting isotope effects resulting from the interplay between isotope equilibrium and photochemical fractionation[47] Previous ambient $\delta^{15}N$-NO_2 studies have successfully tracked the influence of highly variable biogenic soil NO emissions impacting the NO_x budget in a small Midwestern city during the summer[48], suggesting it could be a powerful tool for constraining biogenic soil emissions in the SSAB.

In this study, $\delta^{15}N$ was quantified from NO_2 (and total nitrate, tNO_3) actively collected on a Thermo Scientific™ ChemComb® Speciation Cartridge (CCSC). Ambient NO_2 samples were collected in two locations in the SSAB for 10 months and $\delta^{15}N$ was analyzed to quantify the soil source contributions to the region's NO_x inventories. Using our field measured $\delta^{15}N$-NO_2 values and accounting for nitrogen isotopic fractionation to adjust these values to $\delta^{15}N$-NO_x, we used a mixing model approach to estimate the soil source strength of the field observations based on the mean $\delta^{15}N$-NO_x from each emission source and from the a priori source apportionment reported in CARB's California Emissions Projection Analysis Model (CEPAM) inventory. Because nitrate is influenced by long-range transport, we do not use tNO_3 as a marker for source apportionment. This study aims to improve our understanding of the sources of persistent air pollution in the SSAB by assessing the current NO_x inventory's estimation of soil NO_x emissions.

Methods

Sample collection, extraction, and isotopic analysis

Ambient NO_2 and total particulate nitrate (tNO_3) were collected and quantitatively speciated using a denuder-filter pack active sampling device known as a ChemComb Speciation Cartridge (CCSC), as previously described[49]. Briefly, the body of the CCSC contains an inlet with an impactor plate for the removal of coarse particles, a glass transition piece to induce laminar flow, two honeycomb denuders to collect ambient NO_2 gas, and a downstream filter pack[50]. Denuders were soaked in 10% (v/v) hydrochloric acid (HCl) for 24 h, then rinsed in triplicate with 18.2 MΩ Millipore water and air-dried prior to field preparation. For the collection of NO_2, denuders were coated with 10-mL of 2.5 M potassium hydroxide (KOH) and 25% by weight of guaiacol ($C_7H_8O_2$) using methanol as a solvent, which was allowed to air dry, then capped until assembly for field analysis[51–53]. This mixture selectively binds NO_2 as nitrite (NO_2^-). Following the denuders is a single Nylon

filter (Measurement Technologies Laboratory NY47P, 47 mm and 1 µm pore size) for the collection of tNO_3. Ambient air was sampled at a flow rate of 10 LPM using a mass-flow controller (MKS IE50A008304SBVP20) and vacuum pump. Details about chemicals and materials used can be found in Supplementary Table S1. Field sampling was performed from June 2022 – April 2023 at two sampling sites in the SSAB (Fig. 1), one in the Imperial Valley (Calipatria High School in *Calipatria*, *CA*) and one in the Coachella Valley (Torres-Martinez air station in *Thermal*, *CA*). This project incorporated community engagement and citizen science; Comité Cívico del Valle (CCV), a grassroots community organization based in Imperial County that was founded on the principle that "Informed People Build Healthy Communities", served as our community partners. Trained air monitoring technicians from CCV oversaw field set-up and break-down. Sampling was performed for 3–7 days, approximately monthly over a period of ten months.

The extraction of NO_2 and tNO_3 was performed with 30-mL and 20-mL of MQ water for the front denuder and nylon filter, respectively, then vacuum filtered through a Whatman grade 1 filter. Back denuders were used to check for breakthrough and were not used for isotopic analysis. Field blanks were collected for method validation, however, blanks contained negligible concentrations of NO_2 and tNO_3. Nitrate (NO_3^-) and nitrite concentrations in aqueous solution were determined on a UV-Vis spectrophotometer using a colorimetric method developed by Doane and Horwath (2003) (extraction methods in Text S2)[54]. NO_2 denuder extracts were neutralized with 0.1 M HCl, then isotopic analysis was performed at the UC Davis Stable Isotope Facility by the denitrifier method on a GasBench-PreCon-Isotopic Ratio Mass Spectrometer to determine $\delta^{15}N\text{-}NO_2$[55,56]. The pooled standard deviation for the ^{15}N reference was 0.11‰.

The lifetime of aerosols in the atmosphere is typically 5–10 days, meaning the N in particulate nitrate is derived from a large integrated area that spans several air basins across California. Although there was fair correlation between NO_2 and particulate NO_3 $\delta^{15}N$ values across the experiment (Pearson correlation coefficient of ~ 0.45), the average for the NO_3 samples was ~ 10‰ heavier than for NO_2, indicating that the aerosol nitrate was likely more strongly influenced by distant, traditional fossil-fuel combustion sources of NO_x. Additionally, quantifying isotope effects associated with tNO_3 formation is more difficult[57]. Uncertainty in knowing exactly where the tNO_3 was produced along its long-range trajectory makes it a much more challenging marker for source apportionment studies, therefore we do not use the tNO_3 data (but it is reported in Table 1).

Evaluation of $\delta^{15}N$ references

The isotopic signature of nitrogen is expressed in terms of its $\delta^{15}N$ (per mil, ‰), where:

$$\delta\,^{15}N = (R_{sample}/R_{standard}\ - 1) \times\ 10^3$$

In this equation, R represents the $^{15}N/^{14}N$ ratio. The standard is atmospheric N_2, which is considered to have a globally uniform isotopic composition[58]. Studies of the natural variations in $^{15}N/^{14}N$ ratios from different sources are used to apportion sources of NO_x pollution.

A literature review was conducted to evaluate published stable ^{15}N isotope ratios for various sources of NO_x, and relevant $\delta^{15}N\text{-}NO_x$ values are summarized in Table 2. On average, biogenic soil sources have been observed to have a significantly larger ratio of light ^{14}N isotopes than combustion sources. This phenomenon can be elucidated through the "leaky pipe" analogy, a concept derived from the hole-in-the-pipe model proposed by Davidson and Firestone[32]. In the "leaky pipe" scenario, soil NO-producing processes, such as nitrification, denitrification, and chemodenitrification, act as microbial conduits where microbes preferentially utilize the lighter ^{14}N isotope. This preference arises from kinetic factors that favor the incorporation of the lighter N isotope, leading to a more depleted $\delta^{15}N$ signature[51,58,59]. The "leaky pipe" effect in soils contributes to the observed larger variations reflected in the standard deviations reported in the literature (Table 2 and Supplementary Fig. S4).

It is important to consider the uncertainties of the isotopic signatures for each source due to variations in measurement techniques found in the literature. For this study, passive sampling techniques[60–62] were excluded because the measurement periods were much longer, could allow for a mixture of NO_x sources, and are more

	Calipatria			Thermal		
	$\delta^{15}N\text{-}NO_2$	$\delta^{15}N\text{-}NO_x$	$\delta^{15}N\text{-}tNO_3$	$\delta^{15}N\text{-}NO_2$	$\delta^{15}N\text{-}NO_x$	$\delta^{15}N\text{-}tNO_3$
Jun 2022	− 13.2	− 13.6	− 0.02	No measurements		
Jul 2022	− 13.4	− 14.1	− 2.6	− 14.3	− 16.1	− 4.5
Aug 2022	− 14.4	− 14.9	− 9.8	− 4.6	− 8.0	− 4.8
Sep 2022	− 15.6	− 16.6	− 3.4	− 5.9	− 8.0	N/A
Oct 2022	− 5.3	− 6.1	− 1.1	− 9.7	− 12.0	− 8.2
Nov 2022	− 12.4	− 13.4	− 2.9	1.8	0.2	2.8
Dec 2022	− 13.3	− 14.9	− 2.9	− 7.5	− 9.1	3.4
Jan 2023	− 9.6	− 11.6	− 0.7	− 1.5	− 3.2	3.9
Feb 2023	− 14.8	− 15.5	0.1	− 11.3	− 12.0	2.6
Apr 2023	− 16.0	− 16.0	− 3.4	− 6.8	− 7.6	1.8
Average	− 12.8	− 13.7	− 2.7	− 6.6	− 8.4	− 0.38

Table 1. Field sampling results for $\delta^{15}N\text{-}NO_2$ and estimated $\delta^{15}N\text{-}NO_x$ based on isotopic fractionation calculations, as well as the results for $\delta^{15}N\text{-}NO_3$ for Calipatria and Thermal. All reported units are per mil, ‰.

Source type	$\delta^{15}N\text{-}NO_x$	Mean (‰)	Standard deviation (‰)	References
Mobile source	−8.1‰ to +9.8‰	−2.5	2.7	Walters, Goodwin, et al.[66a], Miller et al.[65]
Biomass burning	−7‰ to +12‰	1.0	4.1	Fibiger & Hastings[45]
Stationary source	−19.7‰ to −13.9‰	−16.5	1.7	Walters, Tharp, et al. (2015)
Biogenic soil emission	−59.8‰ to −14.2‰	−33.2	9.6	Li & Wang[51], Yu & Elliot[59], Miller et al. (2018)

Table 2. Summary of previously reported $\delta^{15}N\text{-}NO_x$ values sorted by emission source type. [a]Only a portion of the measurements from this paper were used since they were measured with a cold, neutral engine, which wouldn't be relevant for ambient temperatures.

	NEI (2020)	CEPAM (2022)			This Study		
Source type	Imperial County (tons/d)	Imperial County (tons/d)	Coachella valley (tons/d)	SSAB total (tons/d)	Imperial County (tons/d)	Coachella Valley (tons/d)	SSAB total (tons/d)
Mobile	11.9 (72.7%)	12.4 (81.8%)	15.9 (88.2%)	28.3 (85.2%)	12.4 (56.7%)	14.7 (69.9%)	28.2 (62.1%)
Biomass burning	0.5 (3.1%)	0.1 (0.9%)	0.7 (4.0%)	0.8 (2.4%)	0.1 (0.6%)	0.6 (3.2%)	0.9 (1.9%)
Stationary	1.3 (8.0%)	1.7 (11.4%)	1.3 (7.4%)	3.0 (9.0%)	1.7 (7.9%)	1.4 (5.9%)	3.1 (6.7%)
Biogenic Soil	2.7 (16.2%)	0.9 (5.9%)	0.1 (0.4%)	1.0 (3.0%)	6.7 (34.7%)	4.7 (21.0%)	11.4 (29.2%)
Total NO_x	16.3	15.2	18.0	33.2	21.8	22.7	45.5

Table 3. The 2022 California emissions Projection Analysis Model (CEPAM) NO_x emission inventory and our estimated soil NO_x adjustments for Imperial County and the Coachella Valley, as well as for the combined SSAB, are shown. The CEPAM inventory is based on an annual average, so we averaged our soil source estimates for our sampling duration. Also shown are the adjustments to the NO_x inventory based on the average results from our field sampling campaign. The EPA's National emissions Inventory (NEI) for 2020 is also shown for comparison for Imperial County only.

difficult to reproduce, ultimately introducing a bias in the $\delta^{15}N\text{-}NO_x$[63]. Additionally, studies on vehicles without catalytic converters were excluded[64] since catalytic converters are mandatory and regulated through California smog checks. For these reasons, only two publications were used to represent mobile source emissions: Miller et al. (2017) and Walters, Goodwin et al. (2015)[65,66]. Not all measured values reported in Walters, Goodwin et al. (2015) were used because some measurements were taken from engines that were cold and/or in neutral. Catalytic converters take a few minutes to warm up and work efficiently, and efficient catalytic converters preferentially remove lighter ^{14}N isotopes[65,66], leading to heavier ^{15}N emissions. Therefore, cold engines are biased with more negative isotopic signatures and likely do not represent background mobile source emissions measured in the Salton Sea Air Basin. Additionally, both studies were performed in the northeastern US in large metropolitan areas where biogenic sources are believed to be negligible. The reported mean from Miller et al. (2017) was then averaged with the mean of warm and/or driven vehicles from Walters, Goodwin et al. (2015) to represent mobile source $\delta^{15}N\text{-}NO_x$ (Table 3). Further, coal burning is not a method of energy production in the Salton Sea Air Basin or surrounding areas, therefore, studies that measured the isotopic signature of NO_x produced through coal combustion have been excluded from our stationary source measurements[64,67].

Soil source strength mixing model estimation and propagation of uncertainty

A best estimate of the sources of NO_x in the SSAB is compiled in the California Air Resources Board's California Emissions Projection Analysis Model (CEPAM) shown in Table 3. CEPAM was used over the EPA's National Emissions Inventory (NEI) because CEPAM is broken into county and air basin, and due to its California focus, should in principle be more accurate. Because chemical and physical processing can induce isotopic fractionation such that $\delta^{15}N$ may not be conserved, isotopic fractionation was calculated to determine $\delta^{15}N\text{-}NO_x$ (see Text S3 and Eq. S1-3)[57,68]. These $\delta^{15}N\text{-}NO_x$ values were then used to calculate the soil source emission strength (E_s) in Eq. 4 based on the average $\delta^{15}N\text{-}NO_x$ of each emission source and based on the a priori source apportionment reported in the CEPAM NO_x inventory, which is used for regulatory modeling in California. Here, δ_{obs} represents the observed $\delta^{15}N\text{-}NO_x$, i represents the main source types accounted for in the CEPAM NO_x inventory (where a, b, c, and s represent mobile, biomass burning, stationary, and soil sources, respectively), α_i represents the proportion each source contributes to the overall CEPAM NO_x inventory, δ_i represents the literature derived $\delta^{15}N\text{-}NO_x$ for each source (Table 3), and E_{inv} represents the total NO_x budgeted in the CEPAM inventory (in tons/d).

$$E_s = \left(\delta_{obs} - \sum_{a,b,c,s}^{i} \alpha_i \delta_i\right) E_{inv} \Big/ \left(\delta_s - \delta_{obs}\right) \quad (4)$$

Equation 1 assumes that the current CEPAM inventory is correct aside from the soil source because the observed $\delta^{15}N$ was (usually) lighter than expected; without adjusting the soil source signature, the CEPAM inventory would indicate a mean $\delta^{15}N\text{-}NO_x$ of -5.04‰ and −3.11‰ for Imperial County and the Coachella Valley, respectively. Therefore, we solve for the magnitude of the soil source such that the observed $\delta^{15}N$ signature can

be explained by the sum of the inventory sources plus the *revised* soil emissions. This procedure further assumes that the sampled NO_2 is entirely from NO_x (or HONO) emitted from sources within the air basin. Figure 1 shows annual NO_2 column data from the European Space Agency's TROPOspheric Monitoring Instrument (TROPOMI) for the year of our sampling.

We propagate the various uncertainties associated with these measurements of sources from the literature to estimate the overall error associated with our calculated soil emissions. Equation 5 comes from the propagation of error for the final soil source strength (σ_{E_s}). The analytical uncertainty δ_{obs} (on average 0.11‰) was ignored because it is an order of magnitude smaller than the standard deviations of the $\delta^{15}N\text{-}NO_x$ measurements for each source (Table 2).

$$\sigma^2_{E_s} = \sum_{a,b,c}^{x} \frac{\alpha_i^2 E_{inv}^2}{(\delta_s - \delta_{obs})^2} \times \sigma_i^2 + \left[\frac{\alpha_s^2 E_{inv}^2}{(\delta_s - \delta_{obs})^2} - \frac{2\left(N - \alpha_s^2 \delta_s E_{inv}^2\right)}{(\delta_s - \delta_{obs})^3} + \frac{N^2 + \alpha_s^2 \delta_s^2 E_{inv}^2}{(\delta_s - \delta_{obs})^4} \times \sigma_s^2 \right] \quad (5)$$

where $N = \left(\delta_{obs} - \sum_{a,b,c}^{i} \alpha_i \delta_i\right) E_{inv}$

Results and discussion

Field sampling results

Results of collected $\delta^{15}N\text{-}NO_2$ signatures are shown in Table 1. Figure 2 displays the soil emission estimates for this field campaign at both sites, comparing the monthly magnitudes to the overall annual CEPAM NO_x inventory. It is apparent that the CEPAM NO_x budget underestimates the soil contribution to ambient NO_x (and consequently to $PM_{2.5}$ and O_3) in both Calipatria (Imperial Valley) and Thermal (Coachella Valley). Soil NO_x contributed 0.3–10.1 (mean: 6.7 ± 3) tons/d and 0–13.8 (mean: 4.7 ± 4) tons/d throughout the duration of the field sampling for the Calipatria and Thermal sites, respectively. These soil emissions amount to on average 11.4 ± 4 tons/d throughout the entire SSAB, an order of magnitude larger than what is represented in the inventory (1.0 ton/d).

The quantitative basis of our estimates relies on the assumption that the ambient NO_2 at the sampling site comes from sources entirely within the SSAB. Figure 1 (and Supplementary Fig. S1) show the overall pattern of column NO_2 observed by TROPOMI during its overpass time near 13:30 local time. The satellite data illustrates two important aspects of the regional NO_x. First, although there is a flow connection between the Coachella Valley and upwind urban sources in the LA basin (Supplementary Fig. S2), the valley plume is distinct and does not appear to simply represent a decaying tail (especially noticeable in the Fall and Winter maps of Supplementary Fig. S1). The Imperial Valley, on the other hand, is only downwind of Mexicali during July/August (Supplementary Fig. S3) and yet it exhibits a broad amorphous shape that deviates from the circular symmetry of a concentration field falling off with distance from an urban core. Second, the basin-wide concentrations are greatest during spring/summer when the photochemical lifetime of NO_x is shortest, supporting our finding that agricultural soil sources are significant, especially during the warmest part of the growing season. Regardless of the details of source apportionment for the sampling, Eq. 4 shows that any influence from urban sources

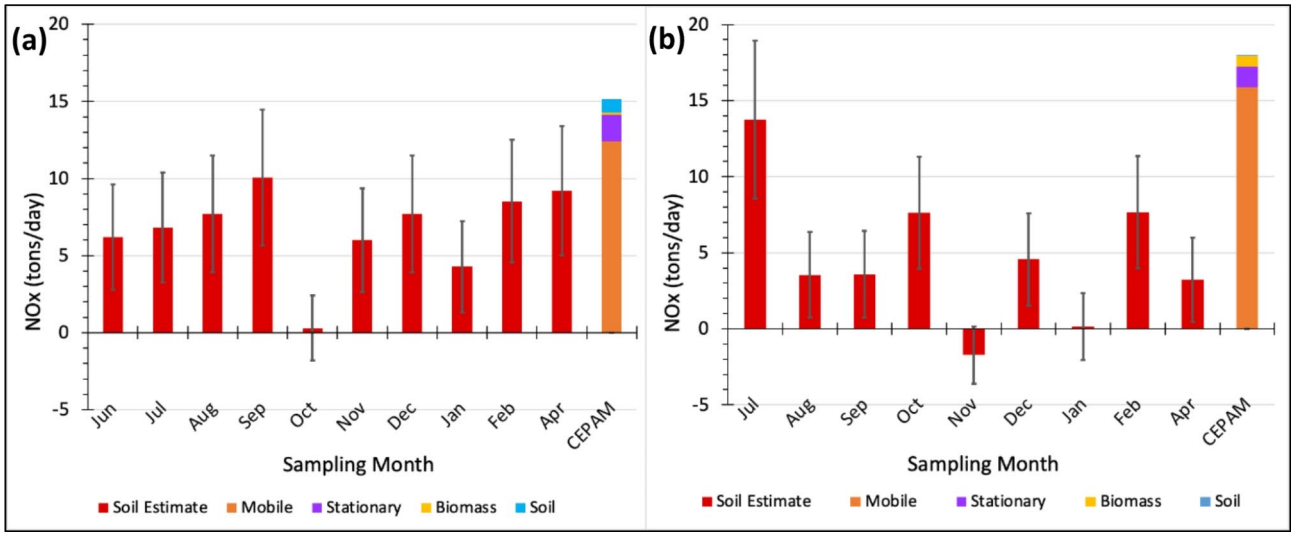

Fig. 2. The NO_x budget (in tons/day) based on CEPAM2019v1.03 for the year 2022 is shown, which is split into mobile, stationary, biomass burning, and soil emission sources for (**a**) Calipatria and (b) Thermal. Soil emission estimates from this study are shown in red, and estimated uncertainties are denoted by the error bars. The annual total CEPAM NO_x inventory for Imperial County (a) and the Coachella Valley (**b**) is presented on the right, where mobile, stationary, biomass, and soil sources are shown in orange, purple, yellow, and blue. Note that in Thermal for the November sampling, there was a negative estimated soil contribution, but we assume that the soil source was zero for this month and justified this assumption due to the error bar range.

upwind (with their heavier $\delta^{15}N$ fractions) would effectively increase our soil emission estimates, meaning that the values reported here represent lower limits. Further details of the regional flow and NO_x advection are discussed in Text S1.

Environmental influences on soil NO_x production

To better understand the environmental influences that control the production of soil NO_x, we look at the leading parameters used in modeling estimates; namely nutrient availability, temperature, and soil moisture[41,69]. Temperature is known to strongly influence soil NO_x production only when soil moisture and nutrient availability are not the limiting factors, although the exact dependence at higher temperatures is still debated[40], and has been observed by satellite over croplands[27]. Nevertheless, no clear temperature dependence was observed in this study (Figs. 2 and 3) despite observations ranging from 17 to 44 °C (Supplementary Tables S3, S4, and Fig. S6). As an agriculturally active desert, NO_x production is likely limited not principally by temperature as in unmanaged landscapes but by nutrient abundance and soil moisture determined by agricultural activity. In addition, the soil microbes in this high-temperature agroecosystem may have acclimated to the extreme desert heat, so their behavior may vary compared to agricultural ecosystems in more temperate regions[42].

The role of soil moisture on the production of NO_x is related to both gas diffusivity and microbial activity, with increasing soil water content stimulating anaerobic conditions and denitrification more. Nitrification, on the other hand, peaks 2–3 days after wetting when the amount of excess water and the rate of downward movement have decreased[42]. In addition, extensive dry periods limit substrate diffusion and cause water-stressed nitrifying bacteria to remain dormant, which allows N substrate to accumulate while temporarily suppressing NO emissions[69–71]. Irrigation reactivates these microbes and redistributes substrate, resulting in NO pulsing events that typically last 1–2 days and can be 10–100 times background emission rates[41,69]. Moreover, soil NO emissions have been shown to spike after all rewetting events, even if fertilizer had not been applied within the last 30 days[42]. To further understand the influence of these parameters, we looked at volumetric soil moisture content using NASA's Soil Moisture Active Passive (SMAP) satellite data. Soil moisture tends to be higher on average in the Imperial Valley agricultural lands than in any other region in the air basin (Fig. 4). This is because of the region's appropriation of approximately 3 billion m^3 of water from the Colorado River, used primarily for frequent irrigation of its ~ 200,000–275,000 ha of arable soil. This is equivalent to ~ 150 cm of water over the croplands whereas the climatological rainfall observed usually only amounts to < 5–10 cm (Supplementary Tables S5 and S6). Due to the amount of agricultural land in the SSAB and uncertainty of irrigation per parcel of land and crop type, it is difficult to accurately estimate the contribution of soil re-wetting on our measurements,

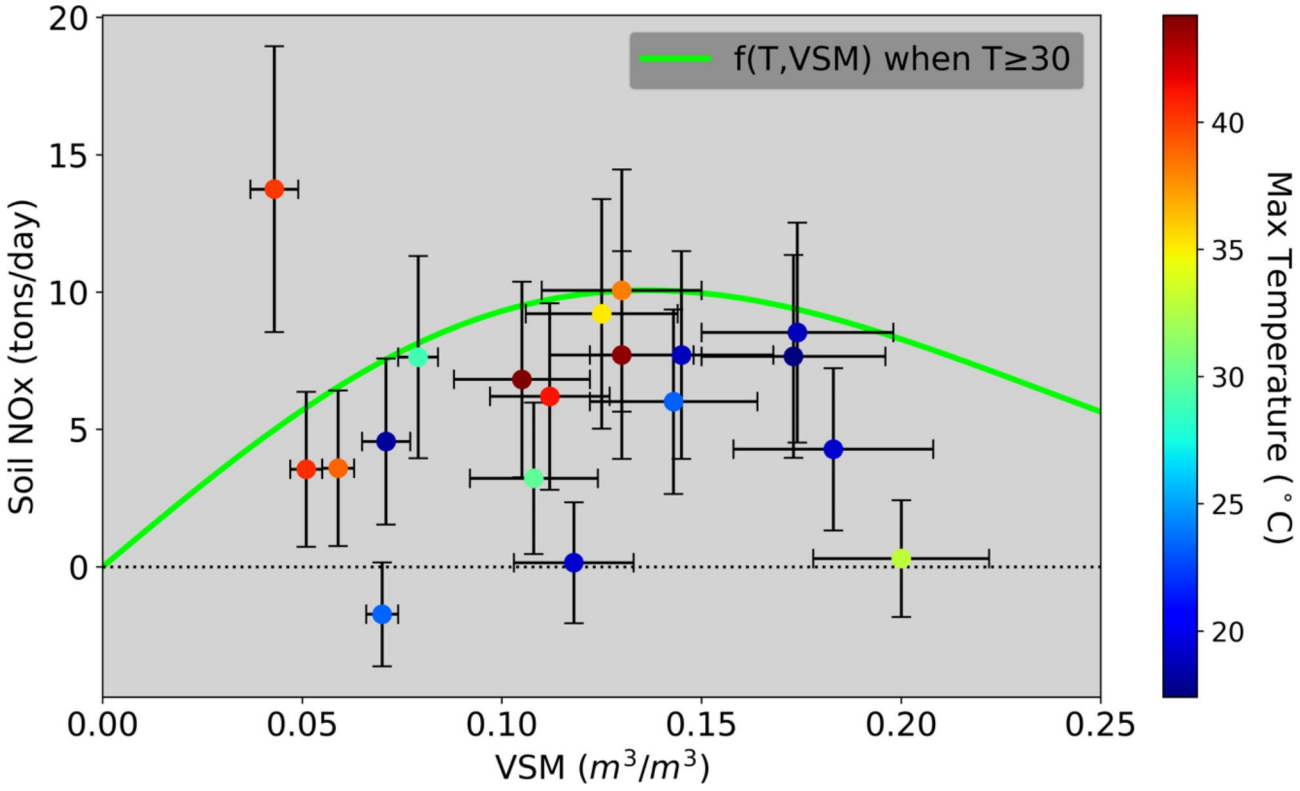

Fig. 3. Soil NO_x estimates from our field campaign compared to the average VSM and maximum temperature during the measurement period. Maximum temperature was determined for the sampling period from the CARB meteorology station at Calipatria and Thermal. VSM was determined for the Imperial Valley for Calipatria measurements and the Coachella Valley for Thermal measurements using SMAP satellite data, filtered for 4:30 pm (closest time to when T_{max} occurs).

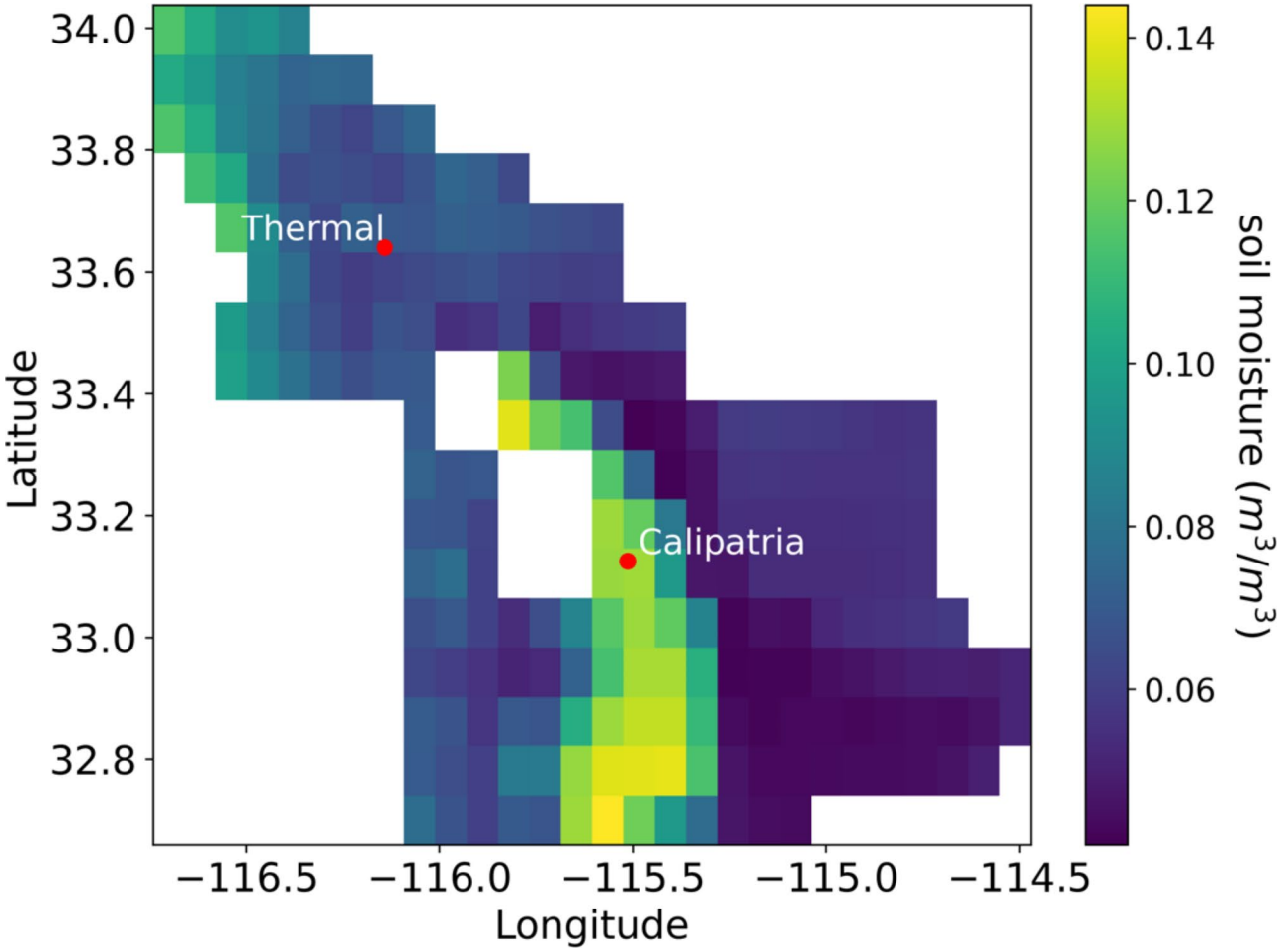

Fig. 4. Average volumetric soil moisture (VSM) for the SSAB from June 2022 – May 2023, obtained from Soil Moisture Active-Passive (SMAP) satellite data.

however this factor likely contributes to our soil NO_x estimates, but it is unlikely that our ~ 10 annual samples captured irrigation variability completely. Furthermore, because the regional distribution of soil NO_x fluxes are highly positively skewed due to these pulsing activities, it is most likely that our ~ 40 days of sampling (Table S2) represents an underestimate to the overall annual sum of emissions, and the mean NO_x concentrations in Calipatria during sampling days was observed to be significantly lower than the annual average (Table S7) further supporting that our estimate of annual emissions in the Imperial Valley is likely a lower limit.

Although Fig. 3 could be interpreted as exhibiting a crude correspondence between soil NO_x emissions and VSM, temperature only appears to be weakly related, which likely indicates that nutrient availability is the dominant factor controlling soil NO_x production in this heavily agricultural region. According to the California Department of Food and Agriculture (CDFA), N fertilizer sales in Imperial County have increased by 137% since 1991[23,72], and an estimated 18-fold since 1930[73], much greater than the national average sevenfold increase. In addition, despite being ranked as the 9th highest in county agricultural sales in the state, Imperial County used more N fertilizer than any other county during 2022 (8% of California total), including the top three crop producing counties (Fig. 5), likely a result of the insufficient nutrient retainment in sandy soils. When N fertilizer is applied in excess, this increases the likelihood that N gases are emitted from the soils. A previous study showed that doubling the fertilization amount from 50 kg N ha^{-1} to 100 kg N ha^{-1} increased the integrated NO_x fluxes by a factor of 5[42].

Spatially and temporally relevant irrigation and fertilization data are not currently publicly available, therefore it is difficult to assess the direct influence of these leading parameters on the soil NO_x emission variance observed in this study. In Fig. 5, we used data from the Trajectories Nutrient Dataset for Nitrogen (TREND-nitrogen) to look at historical N fertilizer applications and legacy N concentrations in Imperial County. N surplus was calculated using TREND-nitrogen, where the county-scale surplus or "legacy" nitrogen (kg N ha^{-1} y^{-1}) is calculated by mass balance from the inputs of atmospheric deposition, fertilizer application, biological N fixation, and human N waste, minus the crop and pastureland N uptake[73]. It is apparent that N fertilizer usage and surplus N in Imperial County has been steadily increasing from 1920 to the present day (Fig. 5). Our estimates are based on a small fraction of days in the Salton Sea Air Basin; in our study, we sampled ~ 39 days in Calipatria and ~ 43 days in Thermal, accounting for about 11% of the year. Inspecting the conditions of our

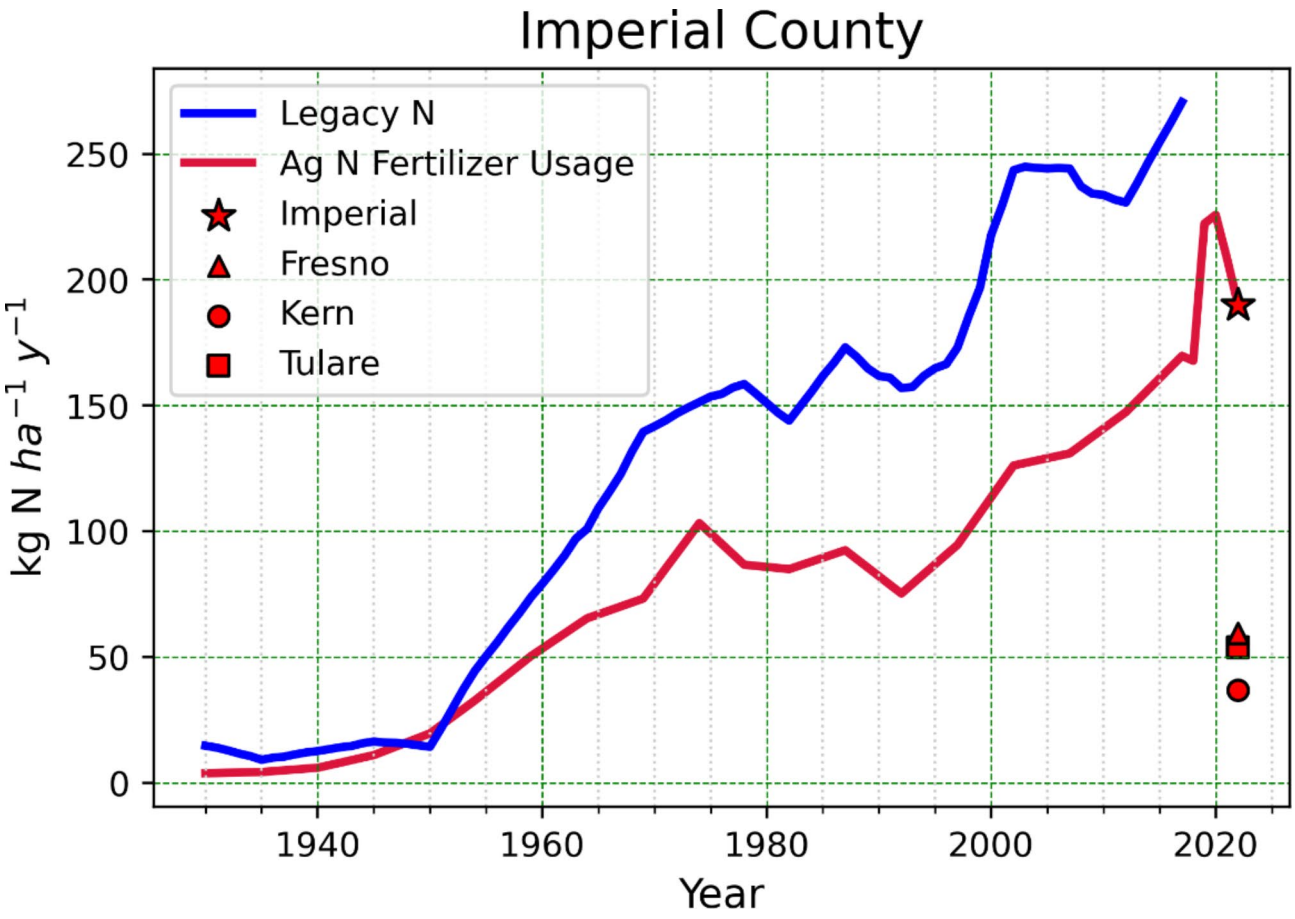

Fig. 5. Imperial County N fertilizer usage (red) and legacy N history (blue) was prepared using the Trajectories Nutrient Dataset for Nitrogen (TREND-nitrogen) from Byrnes et al., 2020. The agricultural fertilizer use was extended after 2017 using the CDFA agricultural statistics for N fertilizer sales. Fresno, Kern, and Tulare Counties are ranked 1st, 2nd, and 3rd in state agricultural sales, while Imperial County is ranked 9th. Fertilizer usages are reported as kg of N used per hectare of agricultural land.

19 sampling intervals with respect to the annual values for VSM and air temperature (Supplementary Fig. S5 and Table S7), they compare well. Nevertheless, without knowing the exact timing of N amendments to all the cropped area, it is possible that while our estimates of annual average VSM and temperature are not statistically different from the average, the soil emissions, predominately influenced by the fertilizer inputs, may be much higher than our estimates having missed many periods of high fertilization in our sporadic sampling.

To understand the overall influence of fertilizer inputs on atmospheric N, we calculated the NO_x flux as a proportion of fertilizer consumption using the net fertilizer usage recorded[23]. Imperial County purchased 57,630 tons of all nitrogen fertilizer, minerals, and compost in 2022[23]. Our annual average soil emission of 6.7 tons NO_x/d in Imperial County implies an average flux of 1.3% of the applied N being released as NO or HONO from agricultural fertilizer inputs. This is squarely within the 0.3–2.5% range reported by Jaeglé et al. (2005). Note that we were unable to quantify this for the Coachella Valley because it is part of the much larger Riverside County and fertilizer sales are only reported county-wide.

Furthermore, $\delta^{15}N$ outliers were observed for October in Calipatria and for November and January in Thermal, yielding estimated soil emissions that were effectively zero within the errors of our measurement technique (Fig. 2). The outliers measured in October (Calipatria) and November (Thermal) correspond to precipitation events during our measurement periods that likely suppressed NO_x emissions during the short intervals of sampling by wetting the soil to excess temporarily (Fig. 6)[41]. During our sampling interval in January (Thermal), precipitation was negligible, but examining HYSPLIT back trajectories for the interval, it appeared that there was a high-pressure system over the region that may have forced subsidence of cleaner tropospheric air into the Coachella Valley, which is consistent with the sampled NO_x being lower than the monthly average by 5.5 ppb (Supplementary Tables S4 and S6). However, this circulation did not persist throughout the entire 5-day sampling period, and the February sample was also collected when NO_x was 5 ppb lower than average, so ultimately, we are uncertain as to the exact cause of this near zero soil emissions measured at Thermal in January.

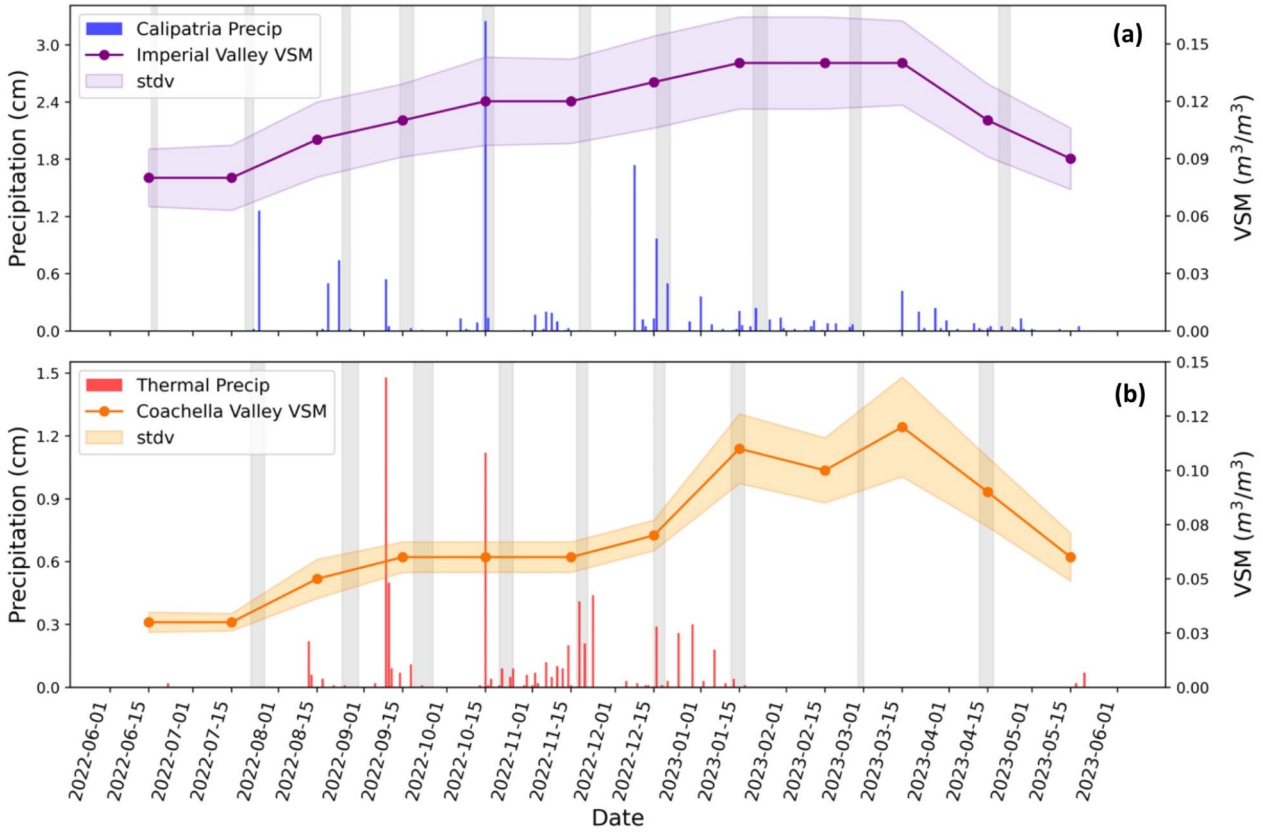

Fig. 6. Monthly average Volumetric Soil Moisture, VSM (2022–2023, shown as a line plot), and the standard deviation (shown with shading) in (**a**) Imperial Valley and (**b**) Coachella Valley compared to the total daily precipitation (2022–2023, shown as bars) at our field sampling sites. Precipitation data was obtained from AQMIS and CIMIS and VSM data was obtained from NASA's SMAP satellite. The grey boxes indicate our sampling dates at each site.

Comparison between studies

To further assess the validity of our results for Imperial Valley, we compared our measurements to Oikawa et al. (2015), which found some of the highest soil NO_x emissions on record from chamber studies across the growing season. They further tested their findings by using WRF-Chem (with soil NO_x emissions calculated using the Model of Emissions of Gases and Aerosols from Nature, MEGAN v2.0) to compare against ambient NO_x measurements from the air quality network. The default soil emissions in the model needed to be enhanced by an order of magnitude to match their chamber measurements more closely, and the enhancement was found to minimize the model's root-mean-square error relative to ambient measurements for one week in September 2012. However, this enhancement still underpredicted tropospheric column densities of NO_2, indicating that there is no single emission factor that can be used to accurately simulate both tropospheric NO_2 columns and surface NO_2 concentrations in the MEGAN parameterization they used.

To compare our integrated valley emissions to other modeled surface fluxes, we used the area of agricultural land in the Imperial Valley to be 270,500 ha based on MODIS satellite land surface characterization[27]. The integrated emissions for their one week in September (the month of our highest estimate of 10.1 ± 4 tons/d) modeled by Oikawa et al. (2015) amounts to 17.2 tons/d (Table 4). That study also attempted to match agreement with satellite NO_2 measurements and found that the emission rate that corresponded best was more like 111.2 tons/day. Their study also found that such soil NO_x emission increases led to concomitant rises in surface level ozone of 2–9 ppb, highlighting the importance of this underestimated source to air quality and the observed disappearance of ozone abatement in the region[9].

We further complied annual average modeled soil NO_x for the Imperial Valley from several other published studies[40,69,70,74,75] that use some version of the common Berkeley Dalhousie Soil NO_x Parameterization (BDSNP) and report them in Table 4. When reading these numbers from large maps of overall emissions, we corrected the fluxes by the factor of 3.9 representing the ratio of the total county area (~1 million ha) to the arable land assuming that the majority of emissions originate from agricultural soils in the region. The study by Wang et al. (2021) proposed a higher emissions parameterization with a temperature plateau that is not reached until 40 °C and compared this to the default parameterization, finding that the new one approximately doubled the emissions for the summer months. Our estimate, 2.5 kg N h^{-1} y^{-1}, falls in between their two results of 1.9–3.8 kg N ha^{-1} y^{-1}. Because the climate in the Imperial Valley is so different from other agricultural regions,

NO_x flux	This study	CARB CEPAM[a]	Jaeglé et al. (2005)[4b]	Hudman et al. (2012)[69b]	Vinken et al. (2014)[75,b]	Oikawa et al. (2015)[42,c]c	Almaraz et al. (2018)[10]	Guo et al. (2020)[78]	Wang et al. (2021)[40,d]	Luo et al. (2022)[77]
tons NO_x day^{-1}	6.7	0.9	4.3	8.5	8.5	17.2–111.2	140.0	1.6	5.2–10.4	13.5
kg N ha^{-1} yr^{-1}	2.5	0.3	6.2	3.1	3.1	6.3–40.6	51.2	0.6	1.9–3.8	4.9

Table 4. Comparing our annual average soil NO_x flux estimate for Imperial County to CARB and other studies. [a]CEPAM2019v1.03 CARB's standard emissions tool for the year 2022 (5.9% of total county NO_x emissions). [b]Corrected from county-wide map estimate to agricultural area assuming majority of emissions arise from cropped soils (county to cropland area ratio of 3.9). [c]Model estimates for September of 2012 to best match satellite and surface network NO_2 observations. [d]Model run for June/July/August 2005–2019; range represents default BDSNP parameterization to proposed higher temperature parameterization.

comparisons must consider that the bulk of the planting occurs between September to April[76]. However, given that our observed estimates for June, July, and August closely match our annual averages, it seems reasonable to compare summer emissions to annual averages. This could occur because nitrogen applications might be at their lowest while soil temperatures are at their highest during these months, with these factors largely balancing each other out.

Almaraz et al. (2018) observed the highest modeled soil NO_x emissions published to date for Imperial Valley[10]. Their method modeled the spatial distribution of soil NO_x emissions using an N isotope model in natural areas and an Integrated Model for the Assessment of the Global Environment (IMAGE) in cropland areas to estimate N losses from soils based on surplus N. Their average NO_x flux estimated for agricultural lands in Imperial County was ~ 140 tons/day (51.2 kg N ha^{-1} yr^{-1}). Our results were also compared to a modeling study performed using an enhanced version of Fertilizer Emission Scenario Tool for the CMAQ (FEST-C) agroecosystem model paired with the Air Pollution Emission Experiments and Policy Analysis (APEEP), further abbreviated as FEST-C*.[77] Data from their 2017 model for Imperial County indicates an annual average soil emission rate of 13.5 tons/day (4.9 kg N ha^{-1} yr^{-1}) about twice as large as our estimate. Finally, Guo et al. (2020) modeled soil NO_x emissions using the DeNitrification-DeComposition (DNDC) model paired with CMAQ, finding the total contribution to the state NO_x inventory was 1.1%.[78] However, they did point out a region of anomalously high emissions in the Imperial Valley, with an annual flux of 0.58 kg N ha^{-1} yr^{-1}. Finally, recent research also suggests the possibility that NO and HONO emissions from drylands[79] and biocrusts[80] could influence air quality to some extent, albeit not as much as the intensive agricultural soils. These studies suggest that such microbial sources could emit as much as 0.1–0.25 kg N ha^{-1} y^{-1}, but from potentially much larger areas across the desert landscape, and thus should be considered in future projections of ambient NO_x (and O_3 and PM2.5).

While there is considerable variability between the various estimates presented (Table 4), undoubtedly in part due to the highly episodic and transient nature of soil NO_x emissions, the CEPAM inventory estimate is consistently much lower than most of the other models and observations. We expect that the dominant control of the instantaneous emission rates is the N amendments made to the agricultural soils daily, so the wide range presented in Table 4 is likely consistent with such inherent variability. Therefore, to obtain an accurate annual average emission rate from soils will take much more comprehensive understanding of N availability in the soils across these highly variable croplands. More work is needed to better constrain the impact of N availability on soil NO_x emissions, as well as the precise soil conditions that control microbial activity and gas-exchange. As of 2022, the Sustainable Groundwater Management Act (SGMA) was modified to require farmers in California to report their daily N inputs for consequences of excess N leaching into groundwater. This emerging data set will be crucial for future studies to investigate soil NO_x emissions in arid agricultural environments and accurately assess its impacts on air quality in rural communities.

Suggestions for future research

While our study does indicate the need for the reassessment of agricultural soil influences on NO_x inventories, especially in high-temperature agroecosystems, there are some aspects of future research that we believe should be prioritized. To better understand the nonlinear relationship of nutrient availability and soil moisture for our higher-than-average NO_x fluxes, having access to publicly available databases that contain spatially and temporally relevant fertilization and irrigation information is crucial. As of 2022, the California Water Resources Control Board now requires farmers to report their fertilizer usage per crop type and acreage as a part of SGMA. However, this information is not currently available to the public. In addition, while fertilizer usage and irrigation data are reported on an annual basis, it is hard to describe the seasonal variability of these factors. We suggest that the state mandate reporting a shorter time interval (weekly to monthly) and make it publicly accessible to support the ongoing study of air pollution from agricultural practices. Understanding the biogeochemical processes that contribute to the production of NO_x (and other nitrogen gases like NH_3, N_2O and HONO) will allow for a better assessment for long-term air quality and climate change, as well as provide insights on agricultural best practices that could be promulgated to improve regional air quality.

It is evident by previous modeling studies that the lack of observational data is significantly hindering the effectiveness of models to produce accurate soil NO_x emissions. Moving forward, there should be more seasonal field analysis of NO_x, HONO, and N_2O emissions from different land/crop types, especially in agricultural systems, since the environmental factors that contribute to N emissions and diffusivity change seasonally and with irrigation/fertilization cycles. These biogeochemical processes are highly complex and influenced by

various factors, including fertilizer type, which models often oversimplify or inaccurately detail. More research needs to be supported in understanding all components of this mechanism, especially fertilizer amount, type, application frequency, irrigation timing, organic carbon availability, soil composition, and pH, in descending order of importance. These studies will improve modeling efforts, hopefully increasing the urgency in addressing these air quality issues, which can be improved with proper management and regulatory efforts.

Moreover, utilizing more complex forms of nitrogen like urea-based fertilizer have been shown to reduce the rate of N diffusivity as NO[42], however, the influence on other air pollutants such as N_2O and other environmental implications need to be better understood. While urea-based fertilizer is typically cheaper, less hazardous, and has a higher nitrogen content (requiring less input), if applied inefficiently it can result in higher N_2O emissions, volatilization of ammonia, and increased acidity in the soil. Oikawa et al. (2015) showed that injecting urea-based fertilizer into the soil rather than applying fertilizer to the top resulted in lower NO emissions compared to dissolved ammonium nitrate, however another study by Thornton et al. (1996) showed high rates of N_2O loss[42,81]. A comprehensive investigation on fertilizer type, application methods, and their environmental implications is crucial to avoid trading NO_x emissions for other, potentially more hazardous environmental issues. Furthermore, the impact of soil NO_x on the production of fine particulate matter, specifically nitrate, is uncertain and is dependent also on ammonia fluxes. To better understand the contribution of agricultural nitrate sources, there must be more research on the impacts of agriculture and controlled animal feeding operations (CAFOs) on the production of both NO_x and NH_3, specifically focused on the impacts of fertilizer usage and waste management. This information is crucial, as most agricultural regions in the state are nonattainment for the $PM_{2.5}$ NAAQS due to the recent lowering of the standard from 12 to 9 $\mu g/m^3$.[82]

Data availability

The isotope data presented in this study are available from the corresponding author upon request. Other data such as meteorology and satellite data is available publicly at the following sites. NO2 column data for Fig. 1 and S1 was obtained from Google Earth Engine using Sentinel-5P NRTI NO2: Near Real-Time Nitrogen Dioxide. The script can be found at: https://developers.google.com/earth-engine/datasets/catalog/COPERNICUS_S5P_NRTI_L3_NO2, and the data was analyzed for June 2022- May 2023 at the Salton Sea Air Basin. The air basin was selected using a https://ww2.arb.ca.gov/geographical-information-system-gis-library. Air quality and mete orological data was obtained from AQMIS (https://www.arb.ca.gov/aqmis2/aqdselect.php and https://www.arb.ca.gov/aqmis2/metselect.php) and CIMIS (https://cimis.water.ca.gov/Default.aspx). The 2022 annual average CEPAM NOx inventory can be found https://ww2.arb.ca.gov/applications/cepam2019v103-standard-emission-tool. Soil Moisture Active Passive (SMAP) data was obtained from NASA's Earth Data Inventory; specifically, we used https://nsidc.org/data/spl4smgp/versions/7. The TREND-nitrogen data set is available https://doi.org/10.1594/PANGAEA.917583.

Received: 10 April 2024; Accepted: 30 October 2024
Published online: 20 November 2024

References

1. Caplin, A., Ghandehari, M., Lim, C., Glimcher, P. & Thurston, G. Advancing environmental exposure assessment science to benefit society. *Nat. Commun.* **10**, 1236 (2019).
2. Fowler, D. et al. The global nitrogen cycle in the twenty-first century. *Philos. Trans. R Soc. B Biol. Sci.* **368**, 20130164 (2013).
3. Hu, L. et al. Global budget of tropospheric ozone: evaluating recent model advances with satellite (OMI), aircraft (IAGOS), and ozonesonde observations. *Atmos. Environ.* **167**, 323–334 (2017).
4. Jaeglé, L., Steinberger, L., Martin, R. V. & Chance, K. Global partitioning of NOx sources using satellite observations: relative roles of fossil fuel combustion, biomass burning and soil emissions. *Faraday Discuss.* **130**, 407 (2005).
5. Miyazaki, K. & Eskes, H. Constraints on surface NO $_x$ emissions by assimilating satellite observations of multiple species: MULTIPLE CONSTRAINTS ON NO $_X$ EMISSIONS. *Geophys. Res. Lett.* **40**, 4745–4750 (2013).
6. Song, W., Liu, X. Y., Houlton, B. Z. & Liu, C. Q. Isotopic constraints confirm the significant role of microbial nitrogen oxides emissions from the land and ocean environment. *Natl. Sci. Rev.* **9**, nwac106 (2022).
7. Stevenson, D. S. et al. Multimodel ensemble simulations of present-day and near-future tropospheric ozone. *J. Geophys. Res.* **111**, D08301 (2006).
8. van Vuuren, D. P., Bouwman, L. F., Smith, S. J. & Dentener, F. Global projections for anthropogenic reactive nitrogen emissions to the atmosphere: an assessment of scenarios in the scientific literature. *Curr. Opin. Environ. Sustain.* **3**, 359–369 (2011).
9. Parrish, D. D., Young, L. M., Newman, M. H., Aikin, K. C. & Ryerson, T. B. Ozone Design Values in Southern California's Air basins: temporal evolution and U.S. background contribution: southern California ozone design values. *J. Geophys. Res. Atmos.* **122**, (2017). 11,166 – 11,182.
10. Almaraz, M. et al. Agriculture is a major source of NOx pollution in California. *Sci. Adv.* **4**, eaao3477 (2018).
11. California Air Resources Board (CARB). Appendix C Coachella Valley Ozone Weight of Evidence Analysis. (2022).
12. Environmental Protection Agency (EPA) & Clean Air, P. 8-Hour Ozone Nonattainment Area Requirements; Determination of Attainment by the Attainment Date; Imperial County, California. *Federal Register* (2008). https://www.federalregister.gov/documents/2020/02/27/2020-03152/clean-air-plans-2008-8-hour-ozone-nonattainment-area-requirements-determination-of-attainment-by-the (2020).
13. Environmental Protection Agency (EPA). PM10 Maintenance Plan and Redesignation Request; Imperial Valley Planning Area; California. *Federal Register* (2020). https://www.federalregister.gov/documents/2020/09/18/2020-18427/pm10-maintenance-plan-and-redesignation-request-imperial-valley-planning-area-california
14. Environmental Protection Agency (EPA). Determination of Attainment by the Attainment Date But for International Emissions for the 2015 Ozone National Ambient Air Quality Standard; Imperial County, California. *Federal Register* (2022). https://www.federalregister.gov/documents/2022/10/20/2022-22276/determination-of-attainment-by-the-attainment-date-but-for-international-emissions-for-the-2015
15. Environmental Protection Agency (EPA). Determination of Attainment by the Attainment Date, Clean Data Determination, and Approval of Base Year Emissions Inventory for the Imperial County, California Nonattainment Area for the 2012 Annual Fine Particulate Matter NAAQS. *Federal Register* (2023). https://www.federalregister.gov/documents/2023/01/11/2022-28278/determination-of-attainment-by-the-attainment-date-clean-data-determination-and-approval-of-base

16. Mendoza, A., Pardo, E. I. & Gutierrez, A. A. Chemical characterization and preliminary source contribution of fine particulate matter in the Mexicali/Imperial Valley Border Area. *J. Air Waste Manag Assoc.* **60**, 258–270 (2010).
17. Census Bureau, U. S. U.S. Census Bureau QuickFacts: Imperial County, California. (2023). https://www.census.gov/quickfacts/fact/table/imperialcountycalifornia/PST045223
18. Miao, Y., Porter, W. C., Schwabe, K. & LeComte-Hinely, J. Evaluating health outcome metrics and their connections to air pollution and vulnerability in Southern California's Coachella Valley. *Sci. Total Environ.* **821**, 153255 (2022).
19. OEHHA. CalEnviroScreen 4.0. (2023). https://oehha.ca.gov/calenviroscreen/report/calenviroscreen-40
20. Comunian, S., Dongo, D., Milani, C. & Palestini, P. Air Pollution and COVID-19: the role of Particulate Matter in the spread and increase of COVID-19's morbidity and mortality. *Int. J. Environ. Res. Public. Health*. **17**, 4487 (2020).
21. Los Angeles Times. California coronavirus cases: tracking the outbreak. *Los Angeles Times* (2023). https://www.latimes.com/projects/california-coronavirus-cases-tracking-outbreak/
22. The New York Times. California Coronavirus Map and Case Count - The New York Times. (2023). https://www.nytimes.com/interactive/2021/us/california-covid-cases.html
23. California Department of Food and Agriculture (CDFA). California Agricultural Statistics Review 2021–2022. (2022).
24. Huang, J. & Hartemink, A. E. Soil and environmental issues in sandy soils. *Earth-Sci. Rev.* **208**, 103295 (2020).
25. Li, H., Tatarko, J., Kucharski, M. & Dong, Z. PM2.5 and PM10 emissions from agricultural soils by wind erosion. *Aeolian Res.* **19**, 171–182 (2015).
26. Moore, K. D. et al. Particulate-matter emission estimates from agricultural spring-tillage operations using LIDAR and inverse modeling. *J. Appl. Remote Sens.* **9**, 096066 (2015).
27. Wang, Y., Faloona, I. C. & Houlton, B. Z. Satellite NO_2 trends reveal pervasive impacts of wildfire and soil emissions across California landscapes. *Environ. Res. Lett.* **18**, 094032 (2023).
28. Ribaudo, M. et al. Nitrogen in Agricultural systems: implications for Conservation Policy. *SSRN Electron. J.* https://doi.org/10.2139/ssrn.2115532 (2011).
29. Spinoni, J. et al. How will the progressive global increase of arid areas affect population and land-use in the 21st century? *Glob Planet. Change*. **205**, 103597 (2021).
30. Intergovernmental Panel on Climate Change. *Climate Change and Land: IPCC Special Report on Climate Change, Desertification, Land Degradation, Sustainable Land Management, Food Security, and Greenhouse Gas Fluxes in Terrestrial Ecosystems* (Cambridge University Press, 2022). https://doi.org/10.1017/9781009157988
31. Williams, E. J. & Fehsenfeld, F. C. Measurement of soil nitrogen oxide emissions at three north American ecosystems. *J. Geophys. Res. Atmos.* **96**, 1033–1042 (1991).
32. Firestone, M. K. & Davidson, E. A. Microbial basis of NO and N2O production and consumption in soil. in *Exchange of trace gases between terrestrial ecosystems and the atmosphere* 7–21 (John Wiley & Sons Ltd., Chichester, UK, (1989).
33. Hall, S. J., Matson, P. A., Roth, P. M. & NOx EMISSIONS FROM SOIL: implications for Air Quality modeling in Agricultural regions. *Annu. Rev. Energy Environ.* **21**, 311–346 (1996).
34. Pilegaard, K. Processes regulating nitric oxide emissions from soils. *Philos. Trans. R Soc. B Biol. Sci.* **368**, 20130126 (2013).
35. Oswald, R. et al. HONO emissions from Soil Bacteria as a Major Source of Atmospheric Reactive Nitrogen. *Science*. **341**, 1233–1235 (2013).
36. Ward, B. B. & Nitrification (2008).
37. Prosser, J. I. The Ecology of nitrifying Bacteria. in Biology of the Nitrogen Cycle 223–243 (Elsevier, doi:https://doi.org/10.1016/B978-044452857-5.50016-3. (2007).
38. Barton, L., McLay, C. D. A., Schipper, L. A. & Smith, C. T. Annual denitrification rates in agricultural and forest soils: a review. *Soil. Res.* **37**, 1073 (1999).
39. Parton, W. J. et al. Generalized model for NO_x and N_2O emissions from soils. *J. Geophys. Res. Atmos.* **106**, 17403–17419 (2001).
40. Wang, Y. et al. Improved modelling of soil NOx emissions in a high temperature agricultural region: role of background emissions on NO2 trend over the US. *Environ. Res. Lett.* **16**, 084061 (2021).
41. Yienger, J. J. & Levy, H. Empirical model of global soil-biogenic NO_y emissions. *J. Geophys. Res. Atmos.* **100**, 11447–11464 (1995).
42. Oikawa, P. Y. et al. Unusually high soil nitrogen oxide emissions influence air quality in a high-temperature agricultural region. *Nat. Commun.* **6**, 8753 (2015).
43. Xue, C. et al. Evidence for strong HONO Emission from Fertilized Agricultural fields and its remarkable impact on Regional O3 Pollution in the Summer North China Plain. *ACS Earth Space Chem.* **5**, 340–347 (2021).
44. Chang, Y. et al. Nitrogen isotope fractionation during gas-to-particle conversion of NOx to NO3- in the atmosphere – implications for isotope-based NOx source apportionment. *Atmospheric Chem. Phys.* **18**, 11647–11661 (2018).
45. Fibiger, D. L. & Hastings, M. G. First Measurements of the Nitrogen Isotopic Composition of NO_x from Biomass Burning. *Environ. Sci. Technol.* **50**, 11569–11574 (2016).
46. Hastings, M. G., Casciotti, K. L. & Elliott, E. M. Stable Isotopes as Tracers of Anthropogenic Nitrogen Sources, Deposition, and Impacts. *Elements* 9, 339–344 (2013).
47. Li, J., Zhang, X., Orlando, J., Tyndall, G. & Michalsi, G. Quantifying the nitrogen isotope effects during photochemical equilibrium between NO and NO2: implications for δ15N in tropospheric reactive nitrogen. *Atmospheric Chem. Phys.* **20**, 9805–9819 (2020).
48. Walters, W. W., Fang, H. & Michalski, G. Summertime diurnal variations in the isotopic composition of atmospheric nitrogen dioxide at a small midwestern United States city. *Atmos. Environ.* **179**, 1–11 (2018).
49. Blum, D. E., Walters, W. W. & Hastings, M. G. Speciated Collection of nitric acid and fine particulate nitrate for Nitrogen and Oxygen stable isotope determination. *Anal. Chem.* **92**, 16079–16088 (2020).
50. Koutrakis, P. et al. Development and evaluation of a glass honeycomb denuder/filter pack system to collect atmospheric gases and particles. *Environ. Sci. Technol.* **27**, 2497–2501 (1993).
51. Li, D. & Wang, X. Nitrogen isotopic signature of soil-released nitric oxide (NO) after fertilizer application. *Atmos. Environ.* **42**, 4747–4754 (2008).
52. Walters, W. W., Simonini, D. S. & Michalski, G. Nitrogen isotope exchange between NO and NO_2 and its implications for $\delta^{15}N$ variations in tropospheric NO_x and atmospheric nitrate. *Geophys. Res. Lett.* **43**, 440–448 (2016).
53. Williams, E. L. & Grosjean, D. Removal of atmospheric oxidants with annular denuders. *Environ. Sci. Technol.* **24**, 811–814 (1990).
54. Doane, T. A. & Horwáth, W. R. Spectrophotometric Determination of Nitrate with a single reagent. *Anal. Lett.* **36**, 2713–2722 (2003).
55. Casciotti, K. L., Sigman, D. M., Hastings, M. G., Böhlke, J. K. & Hilkert, A. Measurement of the Oxygen Isotopic Composition of Nitrate in seawater and freshwater using the Denitrifier Method. *Anal. Chem.* **74**, 4905–4912 (2002).
56. Sigman, D. M. et al. A bacterial method for the Nitrogen Isotopic Analysis of Nitrate in seawater and freshwater. *Anal. Chem.* **73**, 4145–4153 (2001).
57. Bekker, C., Walters, W. W., Murray, L. T. & Hastings, M. G. Nitrate chemistry in the northeast US – Part 1: Nitrogen isotope seasonality tracks nitrate formation chemistry. *Atmospheric Chem. Phys.* **23**, 4185–4201 (2023).
58. Högberg, P. Tansley Review 95 ^{15}N natural abundance in soil-plant systems. *New. Phytol.* **137**, 179–203 (1997).
59. Yu, Z. & Elliott, E. M. Novel Method for Nitrogen Isotopic Analysis of Soil-Emitted Nitric Oxide. *Environ. Sci. Technol.* **51**, 6268–6278 (2017).
60. Ammann, M. et al. Estimating the uptake of traffic-derived NO2 from 15 N abundance in Norway spruce needles. *Oecologia*. **118**, 124–131 (1999).

61. Felix, J. D. & Elliott, E. M. Isotopic composition of passively collected nitrogen dioxide emissions: vehicle, soil and livestock source signatures. *Atmos. Environ.* **92**, 359–366 (2014).
62. Redling, K., Elliott, E., Bain, D. & Sherwell, J. Highway contributions to reactive nitrogen deposition: tracing the fate of vehicular NOx using stable isotopes and plant biomonitors. *Biogeochemistry*. **116**, 261–274 (2013).
63. Dahal, B. & Hastings, M. G. Technical considerations for the use of passive samplers to quantify the isotopic composition of NOx and NO2 using the denitrifier method. *Atmos. Environ.* **143**, 60–66 (2016).
64. Heaton, T. H. E. 15 N/14 N ratios of NOx from vehicle engines and coal-fired power stations. *Tellus*. **42**, 304–307 (1990).
65. Miller, D. J., Wojtal, P. K., Clark, S. C. & Hastings, M. G. Vehicle NOx emission plume isotopic signatures: spatial variability across the eastern United States. *J. Geophys. Res. Atmos.* **122**, 4698–4717 (2017).
66. Walters, W. W., Goodwin, S. R. & Michalski, G. Nitrogen stable isotope composition (δ15N) of vehicle-emitted NOx. *Environ. Sci. Technol.* **49**, 2278–2285 (2015).
67. Felix, J. D., Elliott, E. M. & Shaw, S. L. Nitrogen Isotopic composition of coal-fired power plant NOx: influence of Emission controls and implications for Global Emission inventories. *Environ. Sci. Technol.* **46**, 3528–3535 (2012).
68. Walters, W. W. & Michalski, G. Theoretical calculation of nitrogen isotope equilibrium exchange fractionation factors for various NO y molecules. *Geochim. Cosmochim. Acta*. **164**, 284–297 (2015).
69. Hudman, R. C. et al. Steps towards a mechanistic model of global soil nitric oxide emissions: implementation and space based-constraints. *Atmospheric Chem. Phys.* **12**, 7779–7795 (2012).
70. Jaeglé, L. et al. Satellite mapping of rain-induced nitric oxide emissions from soils. *J. Geophys. Res. Atmos.* **109**, 2004JD004787 (2004).
71. Davidson, E. A. Pulses of nitric oxide and Nitrous Oxide Flux following Wetting of Dry Soil: an Assessment of probable sources and importance relative to Annual fluxes. *Ecol. Bull.* **42**, 149–155 (1992).
72. California Department of Food and Agriculture (CDFA). California Agricultural Statistics Review 1991–1992. (1991).
73. Byrnes, D. K., Van Meter, K. J. & Basu, N. B. Long-term shifts in U.S. Nitrogen sources and sinks revealed by the New TREND-Nitrogen Data Set (1930–2017). *Glob Biogeochem. Cycles* **34**, (2020).
74. Geddes, J. A., Pusede, S. E. & Wong, A. Y. H. Changes in the Relative Importance of Biogenic Isoprene and Soil NOx Emissions on Ozone Concentrations in Nonattainment Areas of the United States. *J. Geophys. Res. Atmospheres* 127, eJD036361 (2022). (2021).
75. *Atmospheric Chem. Phys.* 14, 10363–10381 (2014).
76. UC Davis Agricultural and Resource Economics. Cost & Return Studies. (2004). https://coststudies.ucdavis.edu/
77. Luo, L., Ran, L., Rasool, Q. Z. & Cohan, D. S. Integrated Modeling of U.S. Agricultural Soil Emissions of Reactive Nitrogen and Associated impacts on Air Pollution, Health, and Climate. *Environ. Sci. Technol.* **56**, 9265–9276 (2022).
78. Guo, L. et al. Assessment of Nitrogen Oxide emissions and San Joaquin Valley PM2.5 impacts from soils in California. *J. Geophys. Res. Atmos.* **125**, e2020JD033304 (2020).
79. Eberwein, J. R., Homyak, P. M., Carey, C. J., Aronson, E. L. & Jenerette, G. D. large nitrogen oxide emission pulses from desert soils and associated microbiomes. *Biogeochemistry*. **149**, 239–250 (2020).
80. Weber, B. et al. Biological soil crusts accelerate the nitrogen cycle through large NO and HONO emissions in drylands. *Proc. Natl. Acad. Sci.* **112**, 15384–15389 (2015).
81. Thornton, F. C., Bock, B. R. & Tyler, D. D. Soil emissions of nitric oxide and Nitrous Oxide from Injected Anhydrous ammonium and urea. *J. Environ. Qual.* **25**, 1378–1384 (1996).
82. US EPA. Final Reconsideration of the National Ambient Air Quality Standards for Particulate Matter (PM). (2024). https://www.epa.gov/pm-pollution/final-reconsideration-national-ambient-air-quality-standards-particulate-matter-pm

Acknowledgements

This work was made possible by support from the University of California, Davis (UC Davis) Environmental Health Sciences Center (EHSC) under award number P30ES023513 of the National Institute of Environmental Health Sciences, National Institute of Health. The content is solely the responsibility of the authors and does not necessarily represent the official views of the UC Davis EHSC, nor the National Institutes of Health. Co-funding was also provided by the Western Center of Agricultural Health and Safety via NIOSH grant #U54OH007550. I. C. Faloona's effort was supported by the USDA National Institute of Food and Agriculture, [Hatch project CA-D-LAW-2481-H, "Understanding Background Atmospheric Composition, Regional Emissions, and Transport Patterns Across California"]. We would like to acknowledge our community collaborators. First, this work would not have been possible without the support team at Comité Cívico del Valle (CCV). Additionally, our site in Thermal was located on Torres-Martinez tribal land so we would like to recognize them for their generous use of their air monitoring facility. A special thanks to Joel Craig, William "Jedi" Jeidi, and Diana Navarro for coordinating logistics and helping with set-up. The comments of two anonymous reviewers were helpful in clarifying, extending, and improving this work and we are consequently grateful for their efforts. Early conversations with Cort Anastasio also helped this study immensely.

Author contributions

Conceptualization of the research was done by I.F. and H.L. Methodology was developed by W.W., H.L., and I.F. Data was collected by H.L., I.F., M.M., E.R., C.T., and L.O. H.L. wrote the manuscript with significant input from I.F. and W.W. Funding was acquired by I.F. and H.L.

Declarations

Competing interests

The authors declare no competing interests.

Additional information

Supplementary Information The online version contains supplementary material available at https://doi.org/10.1038/s41598-024-78361-y.

Correspondence and requests for materials should be addressed to I.C.F.